First Demonstration of Single-Mode Distributed Feedback Type-I GaSb Cascade Diode Laser Emitting near 2.9 µm

Mathieu Fradet*[a], Takashi Hosoda[b], Clifford Frez [a], Leon Shterengas[b], Stanley Sander [a], Siamak Forouhar [a], and Gregory Belenky[b]

[a]Jet Propulsion Laboratory, California Institute of Technology, Pasadena, California 91109, USA; [b]Department of ECE, Stony Brook University, Stony Brook, New York 11794, USA

ABSTRACT

We demonstrate GaSb-based laterally-coupled distributed-feedback type-I cascade diode lasers emitting near 2.9 µm as potential sources for OH measurements. The laser heterostructures consist of two GaInAsSb quantum well stages in series separated by GaSb/AlSb/InAs tunnel junction and InAs/AlSb electron injectors. Single-mode emission is generated using second order lateral Bragg grating etched alongside narrow ridge waveguides. The lasers were fabricated into 2-mm-long devices, solder-mounted epi-up on copper submounts, and operate at room temperature. With an anti-reflection coating at the emission facet, the lasers exhibit a typical current threshold of 110 mA at 20 °C and emit more than 14 mW of output power. The Bragg wavelength temperature tuning rate was 0.29 nm/°C.

Keywords: Distributed-feedback, diode lasers, single frequency, GaSb, type-I, laser sensors

1. INTRODUCTION

The hydroxyl radical, OH, is a crucial intermediate in the atmospheres of Earth and Mars. For example, in Earth's atmosphere, the vertical profile of Ozone is controlled by catalytic involving OH radicals [1, 2]. Laser-induced fluorescence (LIF) has been used extensively for lifetime decay measurements of OH in the near ultraviolet [3, 4]. However, semiconductor lasers offer potential break-through OH detection capabilities in the infrared due to their low mass, high output power (tens of milliwatts), reliability, efficiency, and tunability. OH possesses strong absorption features near 2.9 µm that could allow direct measurements of the radical using a tunable laser spectrometer (TLS).

GaSb-based type-I semiconductor diodes have shown reliable operation over a large range of temperature for emission wavelengths as high as 3.4 µm [5]. Cascade pumping of GaInAsSb type-I quantum wells (QW) led to strong increase of continuous wave (CW) output power level and efficiency of lasers emitting near 3 µm [6]. For absorption spectroscopy, CW single-mode emission at room temperature is required. The difficulty of epitaxial regrowth of GaSb-based Al-containing alloys has been a limiting factor in the development of traditional distributed-feedback (DFB) single-mode lasers. Laterally coupled (LC) DFB lasers have been demonstrated to yield single-mode emission without the need for semiconductor regrowth [7]. Metal gratings based on this design have been applied to GaSb-based materials [8, 9]. In order to overcome the additional absorption loss introduced by metal gratings, etched gratings was used to produce GaSb-based LC-DFB, achieving high output power in the 2 to 3 µm regime [10].

In this work we report on GaSb-based type-I two-stage cascade diode lasers using second-order lateral Bragg gratings. These devices have shown to produce single-mode emission near 2.9 µm and generate more than 14 mW of CW emission at room temperature. All the devices were solder-mounted epi-side up on oxygen-free high thermal conductivity copper submounts, the emitting facet was anti-reflection coated, and the back facet was passivated (neutral-reflection coated) to avoid any degradation due to oxidation. These devices exhibited mode-hop free tuning over a broad range of operation between 10 °C to 30 °C.

*mathieu.fradet@jpl.nasa.gov; phone 1 818 354-0546; fax 1 818 393-4773; jpl.nasa.gov

2. DESIGN AND FABRICATION

Type-I cascade diode laser structures were grown by molecular beam epitaxy on Te-doped GaSb substrates. The design was similar to that of two-stage cascade narrow ridge diode lasers producing more than 100 mW at room temperature near 3 µm [11]. The n-type cladding thickness is 2.2-µm while the p-type cladding is 2-µm, composed of AlGaAsSb doped with Te and Be, respectively, with a reduced aluminum content compared to [11], Fig. 1 (a). The reduced aluminum content has two purposes; first it is to increase the refractive index of the cladding layers in order to help achieve a higher coupling of the optical mode to the gratings. Secondly, it is to minimize the tendency of material oxidation by atmospheric exposure after cleaving, thus improving long term reliability. The active region consists of two 12-nm-thick GaInAsSb quantum wells, with an indium concentration of ~50%, separated by a 100-nm-thick graded layer of AlGaAsSb with the composition of Al changing from 50 % down to 5%, and a tunnel junction and electron injector composed of undoped 10-nm-thick GaSb, 2.5-nm-thick AlSb, and 6-period InAs/AlSb Te doped chirped superlattice (SL). A heavily doped p-type GaSb layer was finally grown as a low-resistivity top contact.

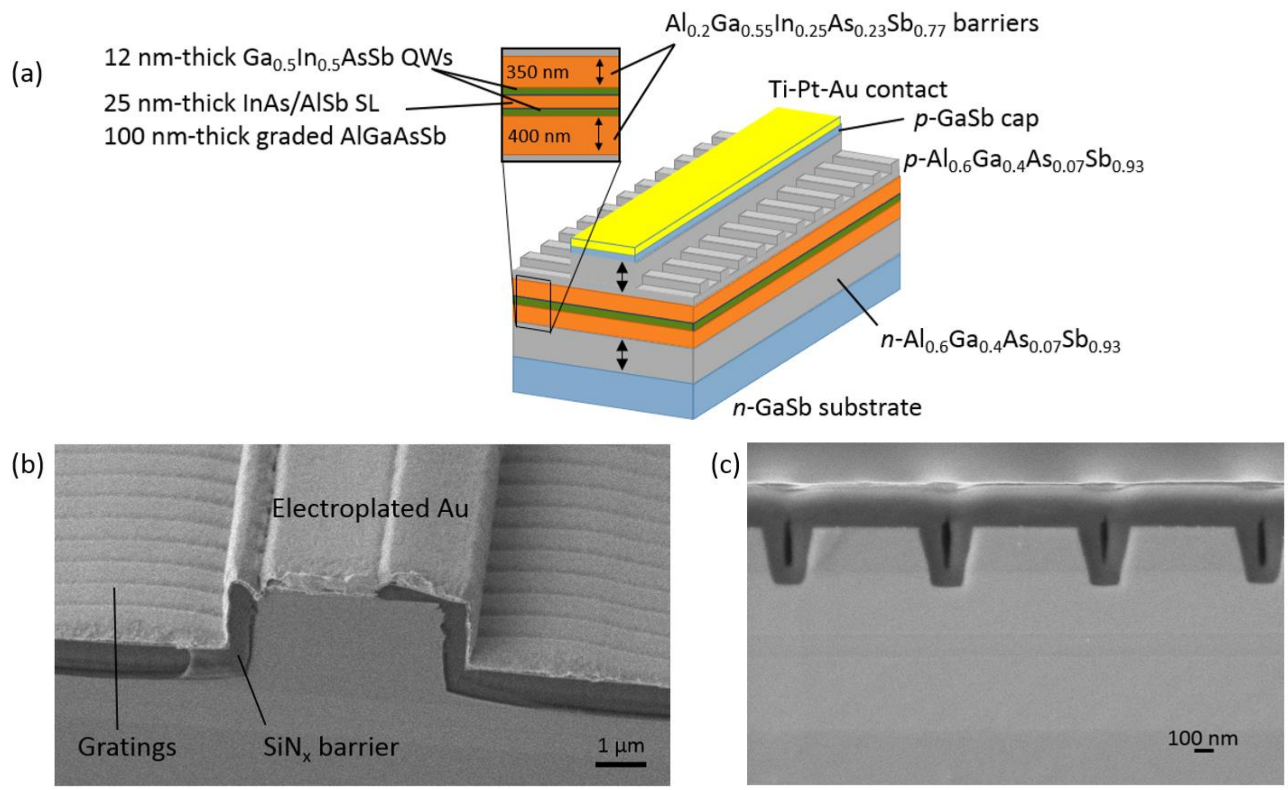

Figure 1. (a) Schematic of the LC-DFB laser structure after etching of the ridge waveguide and the lateral gratings. (b) Scanning electron micrograph of a fabricated laser ridge. (c) Cross section of the laterally coupled gratings, where the gratings have been etched into the waveguide core.

The devices were then processed by first using optical lithography in order to define a narrow-width (~4 µm) ridge waveguide. Using a Cl_2/BCl_3 reactive ion etching (RIE), the waveguide was etched into the p-AlGaAsSb cladding with a silicon nitride (SiN_x) hard mask. This ridge waveguide structure supports only the transverse-electric (TE_{00}) mode at a wavelength of 2.9-µm. Lift-off metallization was used to define Ti/Pt/Au contacts on top of the laser ridges. Using electron-beam lithography, second-order LC-DFB gratings were defined alongside the ridges with a pitch of Λ = 826-nm and then etched into the waveguide core with a similar RIE plasma process. As shown in Fig. 1 (b), we observed a slightly sloped etched surface at the intersection of the ridge sidewalls. This is due to the solid angle limitation over which the neutral etching species near the ridges can reach the semiconductor surface [12]. Consequently, the gratings do not penetrate into the top barrier layer close to the ridge, but do so far from the ridges, as shown in the cross-section scanning electron micrograph (SEM) of the gratings, Fig. 1 (c). The grating etch was then followed by a 400-nm film deposition of SiN_x using plasma-enhanced chemical-vapor deposition. The SiN_x thin-film was then etched away on top of the ridges for electrical contact and a 4-µm-thick Au layer was electroplated on top of the devices for better heat dissipation.

The backside ohmic contact was deposited after the laser wafer was thinned to approximately 100-µm-thick. Rows of devices were cleaved into 2-mm-long bars and using electron-beam evaporation, the front and back facets were coated with a $Y_2O_3/Al_2O_3/Si/Al_2O_3$ anti-reflection (AR) coating, and a Y_2O_3/Al_2O_3 oxide-barrier coating, respectively. Reference substrates allowed us to measure the reflectivity at 2.9 µm for the AR and passivation coatings to be 1% and 30%, respectively. Finally, the lasers were cleaved into individual devices and solder-mounted epi-side up on Au-coated oxygen-free high thermal conductivity (OFHC) Cu submounts using AuSn (10/90) solder.

3. EXPERIMENTAL RESULTS AND DISCUSSION

Mounted LC-DFB cascade diode lasers were tested on a temperature controlled stage for efficient heat extraction. A Molectron thermopile detector was used to measure the optical output power of the lasers, and the spectral characteristics were determined using a Thermo Nicolet FTIR spectrometer at a resolution of 0.125 cm^{-1} with a cooled HgCdTe detector. Figure 2(a) shows current-voltage and light output measurements at different heat sink temperatures for a LC-DFB laser with a cavity length of L = 2 mm. This device can emit over 16 mW of power at 10 °C and 11 mW at 30 °C from the AR coated facet. The near threshold slope efficiency was ~65 mW/A, for a current threshold density ranging from 1.25 kA/cm^2 to 1.56 kA/cm^2. The threshold current density was determined based on the area of the etched laser ridge (~4 µm). However, this constitute an upper bond since current spreading occurs in the unetched active region.

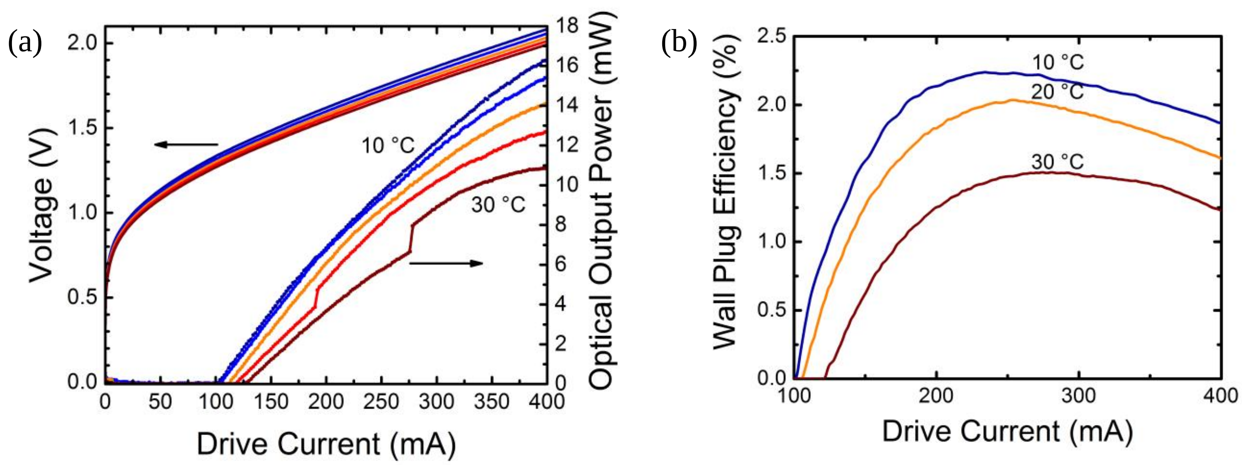

Figure 2. (a) CW light-current-voltage (LIV) characteristics of a 2-mm-long LC-DFB laser at heat sink temperatures from 10 °C to 30 °C by 5 °C increments. The jump in the optical output power emission at 25 °C and 190 mA, and 30 °C and 280 mA is due to the presence of a frequency mode-hop. (b) Wall-plug efficiency of the same 2-mm-long LC-DFB lasers with the facets coated AR-pass.

Figure 2(b) shows the effect of the heat sink temperature on the wall-plug efficiency of the device. These fabricated type-I cascade diode laser can reach an efficiency of over 2.25 % at 10 °C. This represents an improvement of performances compare to a 5 stage interband cascade laser (ICL) structure [13] or GaInAsSb-AlGaAsSb DFB emitting at 2.84 µm [14]. Type-I cascade lasers based on similar heterostructures have been shown to generate in excess of 100 mW near 3 µm for 2-mm-long AR/HR coated epi-side down mounted narrow ridge Fabry-Perot (FP) devices [15]. Figure 2(a) shows the presence of a frequency mode-hop at 190 mA and 280 mA for a heat sink temperature of 25 °C and 30 °C, respectively. This frequency mode-hop is due to the thermal laser gain spectrum shift to longer wavelengths with increasing current. Thus, the DFB mode on red side of stop band becomes dominant, Figure 3. The spectra shown in Fig. 3(a) indicate a nearly constant Bragg wavelength temperature tuning rate of 0.29 nm/°C.

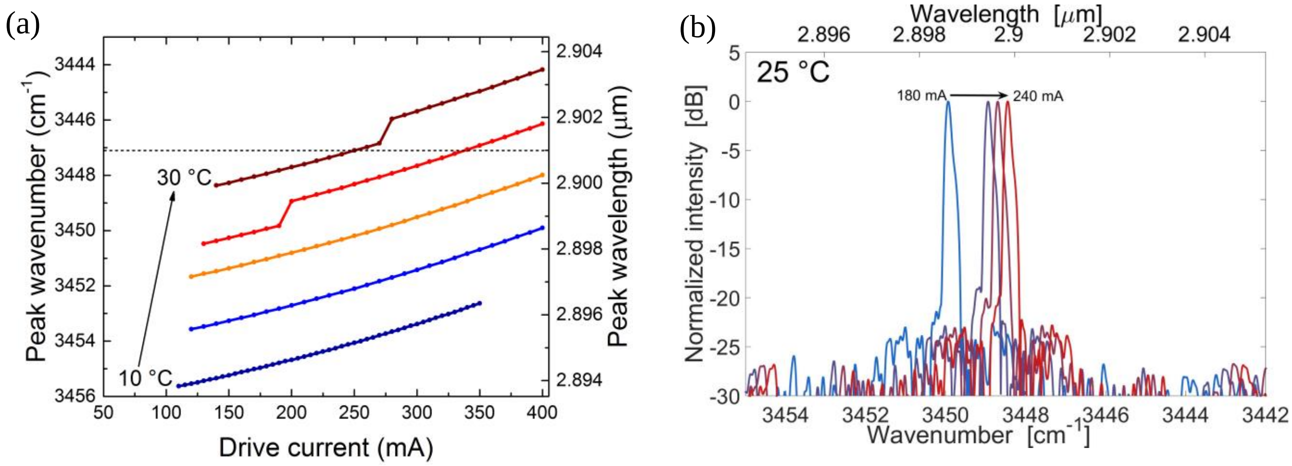

Figure 3. (a) Current and temperature tuning characteristics of the laser emission wavelength near the target OH absorption frequency of 3447.1 cm^{-1}. (b) Emission spectra from a 2-mm-long LC-DFB laser measured at 25 °C with the drive current varied from 180 mA to 240 mA in increments of 20 mA.

The side-mode suppression ratio (SMSR) was observed to be greater than 20 dB for single-mode emission, Fig. 3(b), even after the frequency mode-hop was observed. This corresponds to the noise-limit of the FTIR used for this measurement, single-frequency emission is thus observed even after the mode-hop. As shown in Figure 4, the device can detect OH radicals by tuning the wavelength across an absorption line pair at 2.901 µm (3447 cm^{-1} in wavenumbers) at room temperature and mode-hop-free.

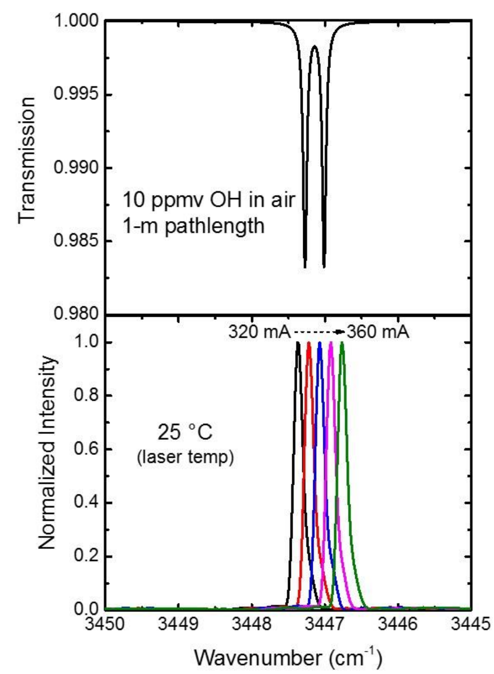

Figure 4. Normalized emission intensity of the device covering OH absorption lines. The OH absorption lines can be hit at 25 °C with drive current between 320 mA and 360 mA.

To achieve high sensitivity for absorption spectroscopy measurements, the light beam is collimated into a multi-pass cell, 30 passes between two Herriott mirrors, where the path length is ~60 meters. The quality of the beam collimation becomes really important, and in order to choose the appropriate mid-IR collimating lenses, the two-dimensional far field of the LC-DFB type-I cascade diodes have been studied as shown in Figure 5(a). The characterization was performed using a cooled HgCdTe detector on a two-axis goniometer and measured a full-width $1/e^2$ divergence angle of 85° and 162° in the horizontal and vertical direction, respectively, relative to the laser ridge. As one could expect for these laser structures, the presence of a fast and slow axis with such high divergence angles require a multi-lens system in order to obtain good collimation over 60 meters of path length without the use of custom-made lenses, which are expensive at those wavelengths.

(a)

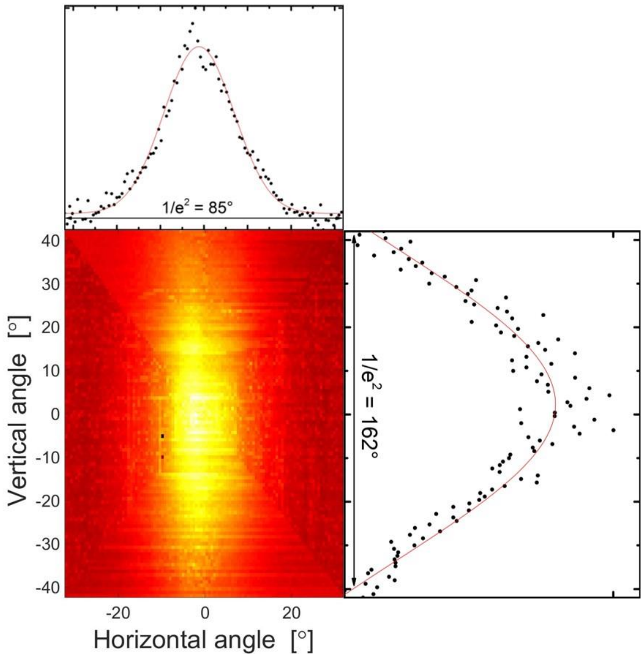

(b)

Figure 5. (a) Measured two-dimensional far-field emission profile of a LC-DFB type-I cascade diode laser with the ridge geometry in Fig. 1. The laser was operated in pulsed mode to allow lock-in amplification of the detector signal in far field. The heat sink temperature was 20 °C, the drive current was 150 mA, with a pulse width of 0.5 µs and a frequency of 10 kHz. Cross sections of the far field intensity are shown with a Gaussian fit. (b) Picture of a TO-3 package used to control the device temperature and current as used in the OH radical absorption measurements setup.

Finally, the diodes were hermetically sealed in TO-3 packages, Fig. 5(b), with internal thermal control for efficient heat extraction by thermoelectric cooler (TEC Microsystems). Due to the highly divergent fast-axis, a wide window is used in order to collect most of the light and collimate it. We used a sapphire window, AR coated and tilted to avoid any back reflections. The OH radical absorption measurements setup uses a series of three external lenses in order to obtain a high quality collimated beam.

4. CONCLUSION

In conclusion, we have demonstrated the viability of LC-DFB type-I cascade diode lasers based on GaSb that emit near 2.9 µm. The laser emission wavelength is targeted for hydroxyl radicals at 2.901 µm (3447 cm^{-1}), capable of emitting 14 mW of single-mode output power at 20 °C and tuning across the wavelength of interest at 25 °C with 12 mW. This is similar performances to GaInAsSb-AlGaAsSb diodes and an improvement over state-of-the-art ICL in this wavelength regime. The use of compact laser packages is suitable with absorption spectroscopy and is a great improvement over LIF on many aspects. Finally, with the improvement of the laser heterostructures that have already led to a narrow-ridge multi-mode emission of over 100 mW, the fabrication of LC-DFB with improved performances around 3 µm will be possible in the near future, and is a viable option over diodes for high power emission.

ACKNOWLEDGEMENTS

The research was carried out at SUNY, supported by US National Science Foundation, grant ECCS-1408126 and US Army Research Office, grant W911NF1110109, and at the Jet Propulsion Laboratory, California Institute of Technology, under a contract with the National Aeronautics and Space Administration.

REFERENCES

[1] Mollner, A. K., Valluvadasan, S., Feng, L., Sprague, M. K., Okumura, M., Milligan, D. B., Bloss, W. J., Sander, S. P., Martien, P. T., Harley, R. A., McCoy, A. B., and Carter, W. P. L., "Rate of gas phase association of hydroxyl radical and nitrogen dioxide," Science 330, 646 (2010).

[2] Nair, H., Allen, M., Anbar, A. D., and Yung, Y. L., "A Photochemical Model of the Martian Atmosphere," Icarus 111, 124-150 (1994).

[3] Matsumi, Y., Kono, M., Ichikawa, T., Takahashi, K., and Kondo, Y., "Laser-Induced Fluorescence Instrument for the Detection of Tropospheric OH Radicals," Bull. Chem. Soc. Jpn. 75, 711-717 (2002).

[4] Stone, D., Whalley, L. K., and Heard, D. E., "Tropospheric OH and HO_2 radicals field measurements and model comparisons," Chem. Soc. Rev. 41, 6348-6404 (2012)

[5] Belenky, G., Shterengas, L., Kipshidze, G., and Hosoda, T., "Type-I diode lasers for spectral region above 3 µm," J. Sel. Top. Quantum Electron. 17, 1426 (2011)

[6] Shterengas, L., Liang, R., Kipshidze, G., Hosoda, T., Suchalkin, S., and Belenky, G., "Type-I quantum well cascade diode lasers emitting near 3 µm," Appl. Phys. Lett. 103, 121108 (2013)

[7] Martin, R. D., Forouhar, S., Keo, S., Lang, R. J., Hunspreger, R. G., Tiberio, R., and Chapman, P. F., "CW performance of an InGaAs-GaAs-AlGaAs laterally-coupled distributed feedback (LC-DFB) ridge laser diode," IEEE Photon. Technol. Lett. 7(3), 244-246 (1995)

[8] Gupta, J. A., Barrios, P. J., Lapointe, J., Aers, G. C., Storey, C., and Waldron, P., "Modal gain of 2.4-µm InGaAsSb-AlGaAsSb complex-coupled distributed-feedback lasers," IEEE Photon. Technol. Lett. 21(20), 1532-1534 (2009)

[9] Salhi, A., Barat, D., Romanini, D., Rouillard, Y., Ouvrard, A., Werner, R., Seufert, J., Koeth, J., Vicet, A., and Garnache, A., "Single-frequency Sb-based distributed-feedback lasers emitting at 2.3 µm above room temperature for application in tunable laser absorption spectroscopy," Appl. Opt. 45(20), 4957-4965 (2006)

[10] Briggs, R. M., Frez, C., Bagheri, M., Borgentun, C. E., Gupta, J. A., Witinski, M. F., Anderson, J. G., and Forouhar, S., "Single-mode 2.65 µm InGaAsSb/AlInGaAsSb laterally coupled distributed-feedback diode lasers for atmospheric gas detection," Optics Express 21, 1317-1323 (2013)

[11] Shterengas, L., Liang, R., Kipshidze, G., Hosoda, T., Belenky, G., Bowman, S. S., and Tober, R. L., "Cascade type-I quantum well diode lasers emitting 960 mW near 3 µm," Appl. Phys. Lett. 105, 161112 (2014)

[12] Keil, D., Helmer, B. A., Mueller, G., and Wagganer, E., "Oxide dual damascene trench etch profile control," J. Electrochem. Soc. 148(7), G383-G388 (2001)

[13] Scheuermann, J., Weih, R., von Edlinger, M., Nahle, L., Fischer, M., Koeth, J., Kamp, M., and Hofling, S., "Single-mode interband cascade lasers emitting below 2.8 µm," Appl. Phys. Lett. 106, 161103 (2015)

[14] Hümmer, M., Rößner, K., Lehnhardt, T., Müller, M., Forchnel, A., Werner, R., Fischer, M., and Koeth, J., "Long wavelength GaInAsSb-AlGaAsSb distributed-feedback lasers emitting at 2.84 µm," Electron. Lett. 42, 583 (2006)

[15] Liang, R., Hosoda, T., Shterengas, L., Stein, A., Ming, L., Kipshidze, G., and Belenky, G., "Narrow ridge $\lambda \approx 3$ µm cascade diode lasers with output power above 100 mW at room temperature," Photon. Technol. Lett. 27. 1041 (2015)